Heliyon 5 (2019) e01867

Contents lists available at ScienceDirect

Heliyon

journal homepage: www.heliyon.com

Bionanocomposite films of agar incorporated with ZnO nanoparticles as an active packaging material for shelf life extension of green grape

Santosh Kumar [a,*], Jyotish Chandra Boro [a], Dharitri Ray [a], Avik Mukherjee [a], Joydeep Dutta [b,**]

[a] Department of Food Engineering & Technology, Central Institute of Technology, Kokrajhar, Assam, 783370, India
[b] Functional Materials, Department of Applied Physics, SCI School, KTH Royal Institute of Technology, SE-164 40, Kista, Stockholm, Sweden

ARTICLE INFO

Keywords:
Food science
Food technology
Nanotechnology
Fruit extract
Zinc oxide nanoparticle
Agar based composite film
Food packaging
Green grape

ABSTRACT

Zinc oxide nanoparticles (ZnONPs) were synthesized by green protocol using *Mimusops elengi* fruit extract as a novel natural resource. The synthesized particles were polyhedral (mostly hexagonal) in shape between 14 - 48 nm with an average size of 24.75 ± 0.78 nm. Nano zinc oxide (ZnO) at concentrations of 2% (w/w) and 4% (w/w), were incorporated into agar matrix. Solution casting method was used to fabricate the bionanocomposite films with ZnONPs in agar. Surface morphology, particle size, crystallinity, thermal stability and functional groups were determined using SEM, TEM, XRD, TGA and FTIR, respectively. Loading of ZnONPs in composite films improved thermal stability, elongation and film thickness, whereas tensile strength and transparency decreased. The films were used for packaging of green grapes, and appearance of the fruit was observed during ambient storage. Grapes packaged in composite films showed fresh appearance up to 14 and 21 days in ambient conditions for 2% (w/w) and 4% (w/w) ZnONPs in films, respectively. The results showed the potential of the fabricated agar-ZnO nanocomposite film as a promising packaging material to enhance postharvest shelf-life of fresh fruits like green grapes.

1. Introduction

Consumer demands for healthy food free from synthetic preservatives, and environmental concerns associated with non-degradable plastic packaging wastes that pollute the ecosystem including water bodies have led to the development of alternative bio-based packaging materials. Bio-based plastics are mainly synthesized from renewable biomass such as polysaccharides and proteins that are attractive alternatives to petroleum-based plastic polymers (Spierling et al., 2018). Natural polymers are inherently biodegradable because of the oxygen or nitrogen atoms in their polymer backbones as opposed to carbon-carbon single bonds predominant in petroleum based polymers. Polysaccharides are abundantly available, are economical and are environmentally friendly biocompatible polymers that are useful raw materials for food packaging applications (Kumar et al., 2017; Kumar et al., 2018; Rhim and Wang, 2013). Among the polysaccharides, agar, commercially harvested from seaweeds, is one of the most common base materials that has been studied extensively (Ali et al., 2017; Khalil et al., 2017; Malagurski et al., 2017a,b). Packaging films developed using agar as biopolymer matrix has good physical properties, as they are transparent, homogeneous and flexible. These properties make it suitable for fabrication of films and coatings for food packaging applications (Orsuwan et al., 2016; Reddy and Rhim, 2014; Santana et al., 2014).

Improvement of physical, mechanical and functional properties of bio-based composites may be achieved by incorporation of inorganic nanoparticles (NPs). There is an increasing interest in zinc oxide nanoparticles (ZnONPs) for food contact application, as this inorganic material has been used in food, pharmaceutics, cosmetics, amongst others (Al-Naamani et al., 2016; Al-Naamani et al., 2017). Zinc oxide (ZnO) is listed in a "generally recognized as safe" (GRAS) material by the Food and Drug Administration (FDA). Zinc is an essential element for human physiological activities, and 10 mg/person/day is needed (EFSA CEF Panel, 2015). ZnONPs are also known to exhibit low toxicity to biological systems (Espitia et al., 2016).

ZnONPs have been synthesized using various physical and chemical methods (Ekthammathat et al., 2014; Rashad et al., 2014; Tee et al., 2016; Tian et al., 2015; Vakulov et al., 2017). Recently, the biological methods for the synthesis of ZnONPs have attracted much attention due to its convenience, lower cost and environment-friendly processes (Chauhan et al., 2011; Govindaraju et al., 2011). Various plants and their

* Corresponding authors.
** Corresponding author.
E-mail addresses: s.kumar@cit.ac.in (S. Kumar), joydeep@kth.se (J. Dutta).

https://doi.org/10.1016/j.heliyon.2019.e01867
Received 5 May 2019; Received in revised form 22 May 2019; Accepted 29 May 2019

parts such as leaf, fruit, peel, flower, seed, latex, etc. are used as reducing agents and stabilizers to control the crystal growth (Bhuyan et al., 2015; Çolak & Karakose, 2017; Davar et al., 2015; Santhoshkumar et al., 2017; Zare et al., 2017). The extracts of various plant parts are rich in polyphenols and amino acids that act as reducing agents and stabilizers, respectively (Stan et al., 2015; Kumar et al., 2016; Kumari et al., 2016).

Mimusops elengi is a medicinal plant belonging to the family Sapotaceae (Mahua-family), and is also named as "Bakul tree" in Sanskrit (an ancient Indian language) (Mitra, 1981). It has been used in traditional medicine for a long time (Baliga et al., 2011). The aqueous extract of flowers, fruits and bark are primarily used for dental ailments (Pyorrhoea, dental caries), as well as for prevention of heart diseases (Shah et al., 2003). The fruit extract of *M. elengi* are rich in polyphenols e.g. ascorbic acid, gallic acid, pyrogallol and resorcinol (Kumar et al., 2014). The objective of the present work was to develop natural antimicrobial films that can be used for the extension of shelf life of fresh produce. Therefore, agar was used as a base material and ZnO nanoparticles as a filler for the fabrication of nanocomposite films. ZnO nanoparticles were used to enhance the functional properties, including mechanical property, of the developed film. The nanoparticles were synthesized by a green protocol using *Mimusops elengi* fruit extract and then incorporated into agar matrix to form the nanocomposite films, which was studied and reported herein. The effectiveness of the developed nanocomposite films was tested by observing changes in appearance of green grapes packaged in the film and stored in ambient conditions.

2. Materials and methods

2.1. Materials

Zinc nitrate hexahydrate, $Zn(NO_3)_2{\cdot}6H_2O$, was procured from Merck Life Science Pvt. Ltd (India), with ≥96.0 % purity. Glycerol ($C_3H_8O_3$) and agar powder were purchased from Avantor Performance Materials Ltd (India) and Sisco Research Laboratories Pvt. Ltd (Mumbai, India), respectively. Fresh fruits of *Mimusops elengi* (Bakul/Maulsiri) were collected from the campus garden of Central Institute of Technology Kokrajhar.

2.2. Preparation of aqueous extract of fruit

The collected fruits of *Mimusops elengi* were washed with double distilled water (ddH_2O), and dried in a shed overnight at room temperature, and then at 70 °C for 24 h in a hot air oven. The dried fruits were ground into a mixer-grinder and then sieved (200 μm) to separate out the finest powder, which was stored in a sealed air tight plastic container for further use. Aqueous extract of the powder was prepared using 4g of fruit powder in 100 mL of dd H_2O. The mixture was heated at 60 °C for 15 min, and then filtered through a Whatman filter paper No.1. The filtrate was centrifuged in a temperature controlled centrifuge at 10,000 rpm for 10 min at 25 °C. The supernatant was collected, labelled and stored at 6 °C until further use.

2.3. Synthesis of ZnO nanoparticles

In a typical synthesis, 10 mL of aqueous fruit extract was taken in five different containers and different amounts (1, 2, 3, 4 and 5 g) of zinc nitrate hexahydrate were added into each container, respectively. The solutions were continuously stirred at 70 °C for 30 min at 500 rpm. Following this, it was placed in a muffle furnace at 400 °C for 2.0 h for the oxidation reaction to occur (Bora et al., 2017). The white powder obtained was pulverized and the resulting fines were stored in a desiccator for further analyses and use.

2.4. Characterization of ZnO nanoparticles

2.4.1. UV-visible spectroscopy

Optical properties of ZnONPs were determined by preparing an aqueous solution using UV-visible spectrophotometer (Perkin Elmer, model λ-35, Waltham, Massachusetts, USA). UV-visible absorption spectra of the samples were measured as a function of amount of leaf extract and reaction time.

2.4.2. Transmission electron microscopy (TEM)

Synthesized particles were studied using a transmission electron microscope (FEI Tecnai, G2 20, Hillsboro, Oregon, USA) working at an acceleration voltage of 200 kV. A drop of aqueous solution of ZnO nanoparticles (sample prepared with 1 g $ZnNO_3.6H_2O$) was put on holey-carbon coated copper grid of 300 meshes. The excess solution was removed using a blotting paper, following which the grid was allowed to dry at room temperature prior to TEM measurements.

2.4.3. X-ray diffraction (XRD) analysis

Crystal structure of synthesized particles was determined using X-ray diffractometer (XRD-6000, Shimadzu, Japan) operated at 40 kV and 30 mA with Cu Kα radiation (wavelength - 0.15406 nm). The crystalline domain size was estimated from the width of the XRD peaks, using the Debye-Scherrer formula, $D = K\,\lambda/\beta\,\cos\theta$; where, D is the average crystallite domain size perpendicular to the reflecting planes, K is the crystallite shape factor (approximated as 0.94 since the particles were polyhedral as will be discussed later in the results and discussion section), λ is the X-ray wavelength, β is the full width at half maximum (FWHM) and θ is the diffraction angle.

2.4.4. Development of Agar-ZnO nanocomposite films

Molten agar (100 mL; 2.5 %) was prepared by dissolving 2.5 g of agar powder in 100 mL of dd H_2O in three separate beakers, which were heated at 90 °C for 1.0 h upon continuous stirring at 1000 rpm. 50 mg and 100 mg of ZnONPs (synthesized by adding 1 g of $ZnNO_3.6H_2O$ in 10 mL of aqueous fruit extract) were added into two of the beakers with 2 % (w/w) and 4 % (w/w) of agar, respectively. Control sample was prepared in the third beaker without adding any nanoparticles. The samples were further heated and mixed at 90 °C for 30 min at 1000 rpm. 0.75 g of glycerol was added in all the three sample mixtures at the rate of 30 % (w/w) of agar, as a plasticizer. The mixtures were then heated till they became sticky liquid, and 15 mL of this final film forming solution (FFS) solutions was immediately poured on glass Petri-dish of dimension (100 × 15 mm). The samples were allowed to settle at room temperature for 24 h, and then dried in an oven at 40 °C for 2.0 h. The prepared films were removed from glass plates, and were allowed to stay at ambient conditions for 2.0 h. Finally, the films were stored in airtight plastic bags until further use.

2.5. Characterization of composite films

2.5.1. Film colour and transparency

Surface colour of the packaging film is an important parameter for food packaging applications, as it influences the general appearance and consumer acceptability. The colour and opacity of the film samples were evaluated using a Chroma Meter ($D25L^T$, HunterLab, USA) to measure L*, a* and b* values. A white standard color plate (L* = 91.33, a* = -1.12 and b* = -2.05) was used as background. The total colour difference (ΔE) values of the samples were calculated using the following equation: $\Delta E = [(\Delta L)^2 + (\Delta a)^2 + (\Delta b)^2]^{0.5}$. The transparency of the film samples were compared by using a green colour background during the image capture in the microscope. Values for each of the samples were the averaged over five replicates.

2.5.2. Measurement of thickness and textural properties of nanocomposites

Mechanical properties such as tensile strength (TS) and extensibility

of films are important parameters to assess its ability to maintain integrity against environmental stress factors associated with packaging applications. Mechanical properties of the developed nanocomposite film samples were determined by quantifying the tensile strength (TS) and percentage elongation at break (EAB). Texture analyzer (Stable Micro Systems Ltd, TA. XT plus, UK) equipped with a 0.5kN load cell was used to measure tensile strength and percentage elongation at break according to the ASTM standard method. Film samples of 2.54 × 6.0 cm dimension were cut, and used in the analysis. The thickness of the film samples was measured using a hand-held digital micrometer (Mitutoyo Corporation, Japan).

2.5.3. Fourier-transform infrared (FTIR) spectroscopy

FTIR analysis of the agar nanocomposite and the control films was performed using Fourier-transform infrared spectrophotometer (Perkin Elmer, Model-FTIR Spectrum 2, Waltham, Massachusetts, USA). FTIR spectra were recorded in the wavelength range of 4000–500 cm^{-1}, and were used to determine the presence of functional groups and interactions among various components of the film samples.

2.5.4. Microstructure and elemental analysis

Scanning electron microscopy (SEM) was performed to observe the microstructure of the agar nanocomposite and control film samples. Small piece of film sample was mounted on a SEM specimen holder and analyzed using a field emission scanning electron microscopy (FE-SEM, Carl Zeiss, Model Supra 55, Oberkochen, Germany) working at an accelerating voltage of 20 kV.

2.5.5. Thermogravimetric (TGA) analysis

Thermal stability of the developed films was studied in a thermogravimetric analyzer (STA-6000, PerkinElmer, Massachusetts, USA). Film samples (1.0 g approx.) were heated at a temperature range of 30–600 °C at a heating rate of 10 °C/min in nitrogen atmosphere (50 cm^3/min) and the weight loss of the samples were recorded as a function of temperature.

2.5.6. Application of the developed film in packaging of fruit

The developed composite films were studied to test shelf life extension of green grapes. Fresh green grapes of approximately similar size, shape, maturity and colour were purchased from local market, and 25 grapes were wrapped with the each composite film sample. One set of 25 grapes was wrapped with plastic (polyethylene) film as a control. The wrapped fruit samples were kept in ambient conditions to simulate the conditions, in which they are kept by local vendors and retailors, and the packaged fruits were regularly observed up to 25-days.

3. Results & discussion

3.1. Characterization of ZnONPs

The synthesized NPs were polyhedral (mostly hexagonal) in shape as observed in the transmission electron micrograph (Fig. 1). It is evident

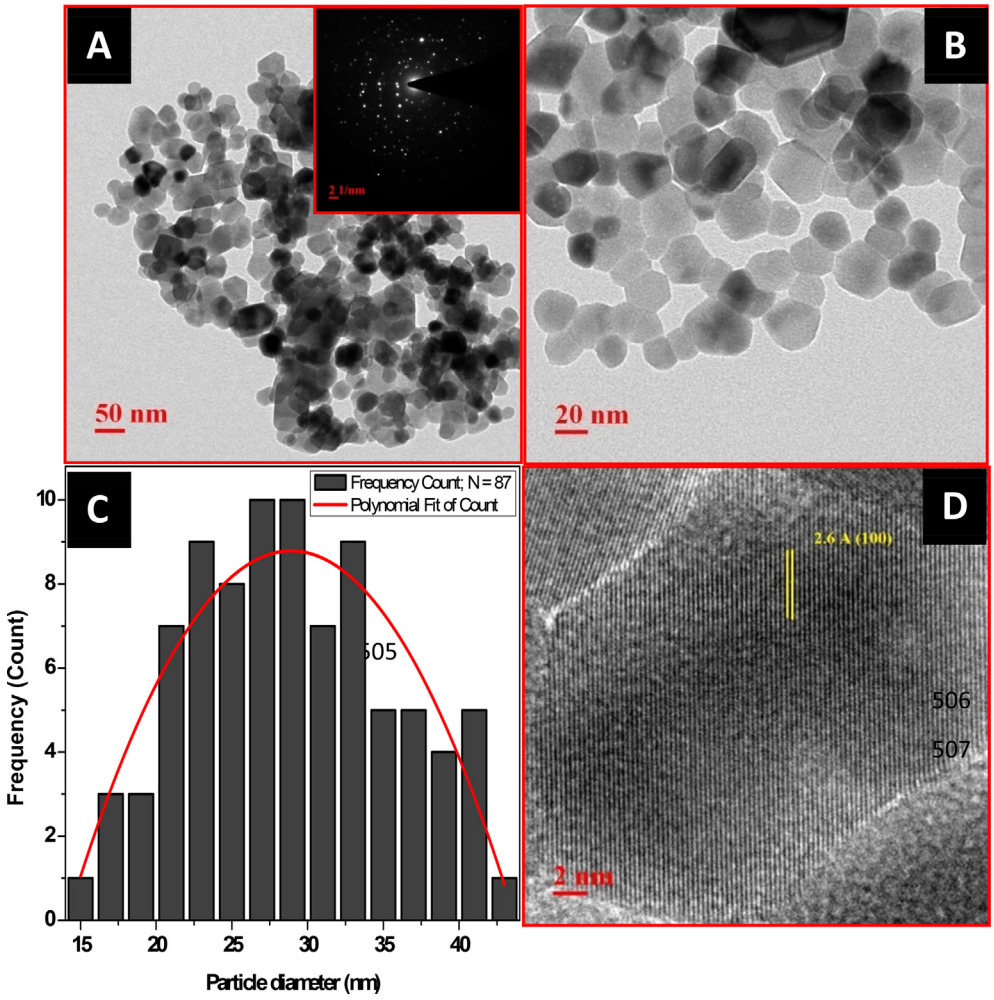

Fig. 1. (A–B) Transmission Electron micrographs (TEM) of synthesized ZnONPs at different magnifications (Inset of Fig. 1A, SAED pattern) (C) particle size distribution histogram, and (D) High Resolution Transmission Electron micrographs (HRTEM) images with indicated lattice spacing.

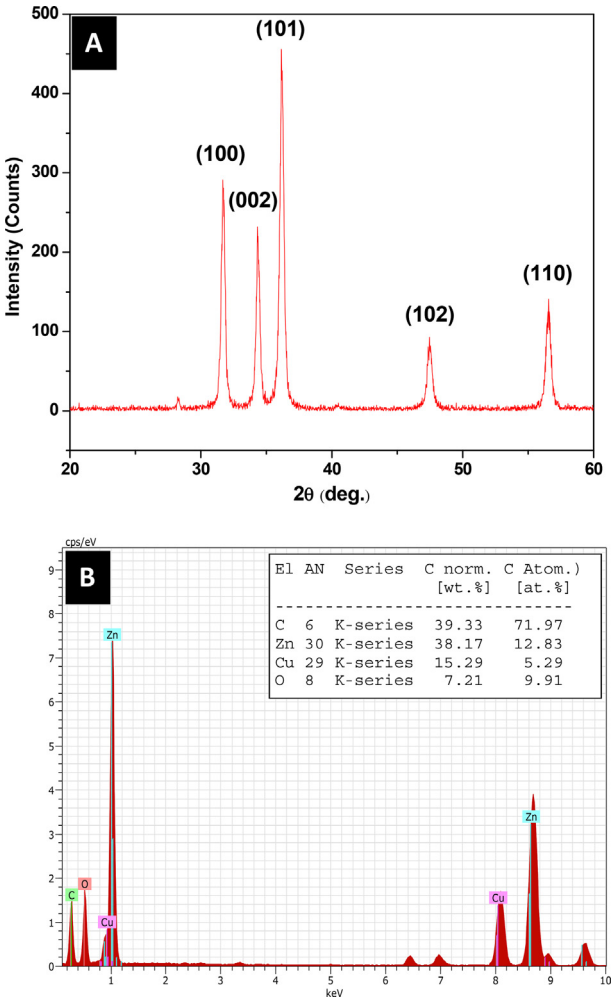

Fig. 2. (A) Typical X-Ray diffraction (XRD) of synthesized nanoparticles, and (B) EDS spectra of the bio-synthesized ZnONPs (Inset; Quantitative elemental analysis).

from particle size distribution histogram (Fig. 1C) that the synthesized NPs are in the size range of 14–48 nm with an average size of 24.75 ± 0.78 nm. Selected area electron diffraction (SAED) patterns from the samples (inset of Fig. 1A) showed that the nanoparticles were crystalline and randomly orientated. The diffraction rings could be indexed as (100) (002) and (101) reflections, corresponding to hexagonal lattice associated with the wurtzite structure of ZnO. Furthermore, a fringe d-spacing of 2.6 Å corresponding to (100) plane that is associated with the hexagonal structure of ZnO could be observed in high resolution transmission electron micrograph (HRTEM) (Fig. 1D).

Typical X-Ray diffractogram of synthesized nanoparticles (Fig. 2A) matched well with the hexagonal phase of JCPDS (card no.0-3-0888), and no indication of secondary phases or impurities were observed. The strong and narrow diffraction peaks indicated good crystalline structure of the particles. The sharp intense diffraction peaks appearing at about 2θ of 31.68, 34.28, 36.28, 47.47 and 56.57° correspond with those from (100) (002) (101) (102) and (110) orientations, respectively confirming the wurtzite crystalline phase of ZnO, which confirms the observations made by SAED analysis as discussed above. Average crystalline size of the synthesized nanoparticles was 23.94 nm, as calculated by using the Debye-Scherrer formula. The result is in good agreement with that of the TEM analysis. Electron diffraction spectra (EDS) (Fig. 2B) of the sample showed that C, Zn, Cu and O were present (C and Cu from the carbon coated copper grid). Thus, the synthesized ZnONPs were pure, as no other elements could be found in the sample. According to EDS report, the weight percentage and atomicity of C, Zn, Cu and O were 39.33, 38.17, 15.29, 7.21 and 71.97, 12.83, 5.29, 9.91, respectively (inset of Fig. 2B).

3.2. Agar-ZnO nanocomposite films

3.2.1. Surface colour and transparency of the films

The macroscopic images of the agar–ZnO nanocomposite and the control films are shown in Fig. 3. The colour parameters (L*, a*, b* and ΔE values) of the films are summarized in Table 1. The transparency of the films was found to reduce with increasing concentration of ZnONPs in the nanocomposites due to higher scattering from the nanoparticles (Malagurski et al., 2017a,b). L*-values of the films increased slightly and a*-values increased significantly, while significant reduction in b*-values were observed with increasing ZnONPs in the nanocomposite film. These results indicated that the lightness of the film samples increased with decrease in greenness and yellowness upon incorporation of ZnONPs. The total color difference (ΔE) values of the nanocomposite films decreased compared to the control film. The ΔE value of the control was 18.11 ± 0.29 that reduced to 12.79 ± 0.33 and 8.32 ± 0.26 upon addition of ZnONPs @ 2% (w/w) and 4% (w/w), respectively.

3.2.2. Textural properties of the nanocomposite films

The thickness and mechanical properties of the agar-ZnONPs composite and control films are shown in Table 2. The thickness of the control film was 54.87 μm, whereas it increased to 75.33 and 77.34 μm upon incorporation of ZnONPs @ 2 % (w/w) and 4 % (w/w), respectively. Loading of ZnO nanoparticles led to increase in viscosity and thus increased film thickness. The results showed that tensile strength (TS) decreased, whereas percentage elongation-at-break (EAB) increased with higher ZnONPs loading in the composite films. The TS of the control film was 51.02 MPa that reduced to 29.19 MPa and 20.68 MPa, respectively, after incorporation of ZnONPs @ 2 % (w/w) and 4 % (w/w). The EAB of

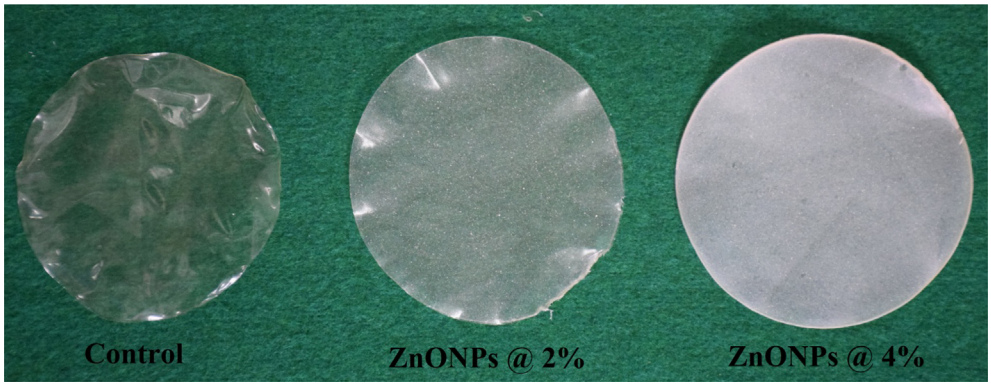

Fig. 3. Photographs of the ZnONP-agar nanocomposite films.

Table 1
Optical properties of the agar-ZnO nanocomposite films.

Film samples	L*	a*	b*	ΔE
Only agar (control) film	$86.74^{a} \pm 0.93$	$-1.56^{a} \pm 0.53$	$15.47^{a} \pm 0.82$	$18.11^{a} \pm 0.29$
Agar–ZnONP @ 2% (w/w) film	$89.24^{a} \pm 1.28$	$-2.23^{a} \pm 0.41$	$9.81^{b} \pm 1.54$	$12.79^{b} \pm 0.33$
Agar–ZnONP @ 4% (w/w) film	$89.30^{a} \pm 1.76$	$-2.78^{a} \pm 0.38$	$5.84^{b} \pm 2.41$	$8.32^{c} \pm 0.26$

Results were represented as means of replicates±standard deviations. Values with different superscript letters in the same column mean significant difference between treatments ($p < 0.05$).

Table 2
Tensile properties and thickness of the only agar and agar-ZnO nanocomposite films.

Film samples	Thickness (μm)	TS (MPa)	EAB (%)
Only agar (control) film	$54.87^{a} \pm 3.4$	$51.02^{a} \pm 1.5$	$27.90^{a} \pm 0.6$
Agar–ZnO @ 2% (w/w) film	$75.33^{a} \pm 2.7$	$29.19^{b} \pm 0.9$	$32.63^{ab} \pm 1.1$
Agar–ZnO @ 4% (w/w) film	$77.34^{a} \pm 4.1$	$20.68^{b} \pm 2.3$	$37.23^{b} \pm 1.9$

Results were represented as means of replicates±standard deviations. Values with different superscript letters in the same column mean significant difference between treatments ($p < 0.05$).

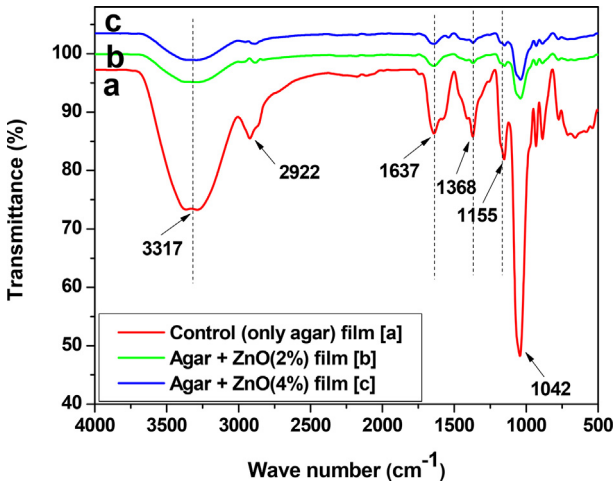

Fig. 5. Fourier Transform Infrared (FTIR) spectra of the nanocomposite films compared with agar film.

the control film was 27.90 ± 0.6% that increased to 32.63 ± 1.1% and 37.23 ± 1.9%, respectively, upon addition of ZnONPs @ 2 % (w/w) and 4 % (w/w). The significant differences in TS and EAB upon the incorporation of ZnONPs in the nanocomposites suggest morphological and

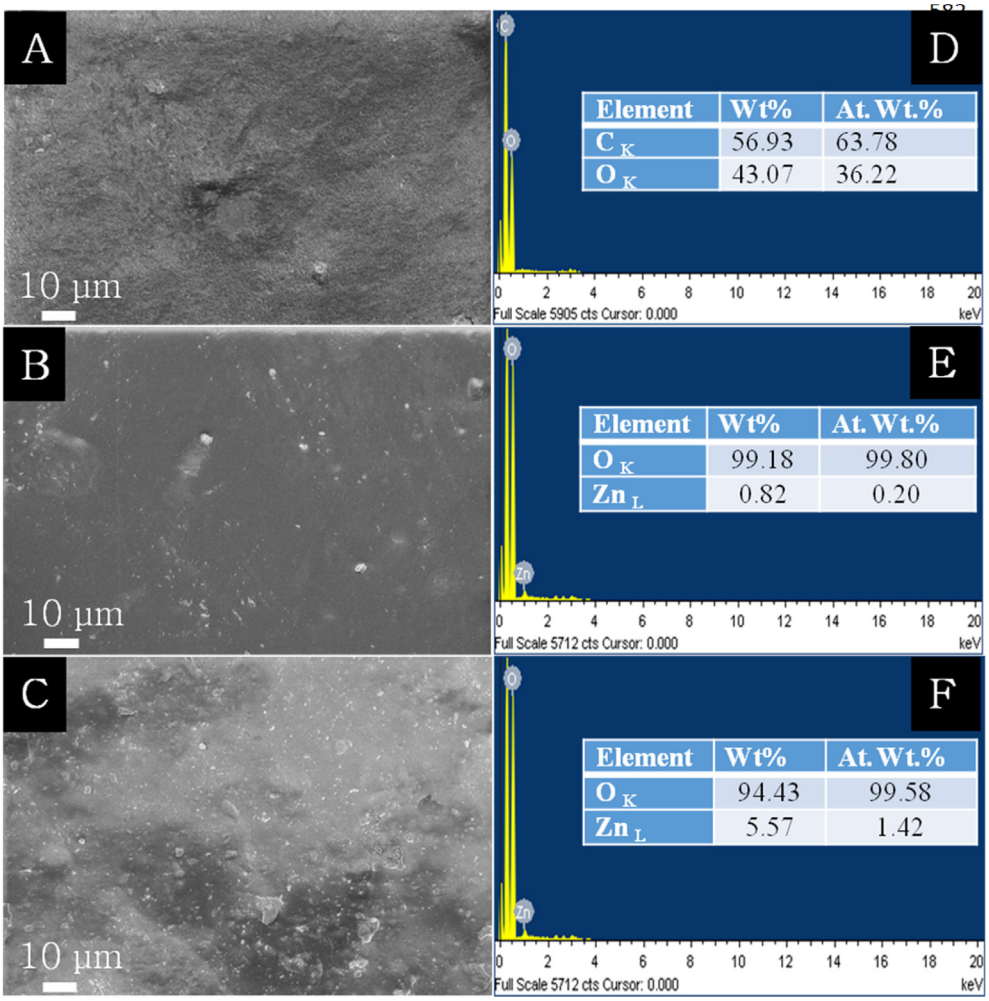

Fig. 4. SEM micrographs of the films (A) Control (B) Agar-ZnO @ 2% (w/w) (C) Agar-ZnO @ 4% (w/w) and EDX spectra of the films (D) Control (E) Agar-ZnO @ 2% (w/w) (F) Agar-ZnO @ 4% (w/w) [The quantitative elemental analysis of the each film is given in the inset of their respective EDX spectrum].

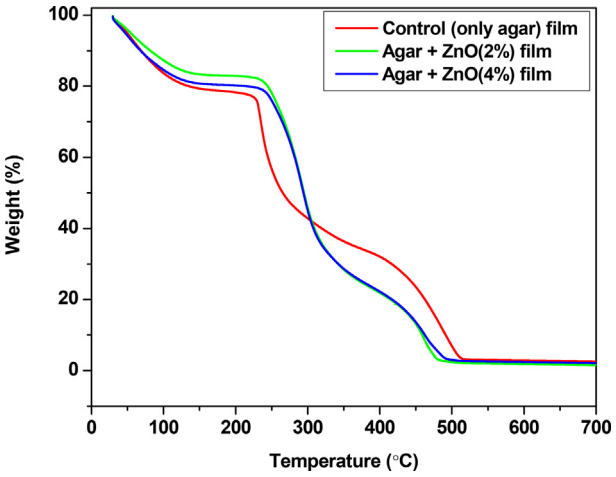

Fig. 6. TGA curve of ZnONP-agar nanocomposite films.

structural changes in the biopolymer matrix.

3.2.3. *Surface morphology of the films*

Scanning electron micrographs of typical agar-ZnO nanocomposite films are shown in Fig. 4. The presence of the ZnONPs on the film surface is clearly visible which are evenly distributed across the films as observed in SEM images (Fig. 4B & C). Also, the surface of the composite film is rather smooth, compact and heterogeneous compared to that of the control film. Some agglomeration of nanoparticles was observed in films with higher concentrations of ZnONPs (Fig. 4C). The size of ZnONPs agglomerates in the polymer matrix increased with increase in amount of NPs. It was also observed that the nanoparticles strongly adhered to the agar matrices, which led to the modification in the physical and chemical characteristics of the films. Fig. 4D, E & F illustrate the EDX spectrum of the control and the agar-ZnO nanocomposite films. The EDX profile was acquired on a single spot of the composite film samples. In the control film, only carbon and oxygen were detected, whereas, oxygen and zinc were present in the nanocomposite films.

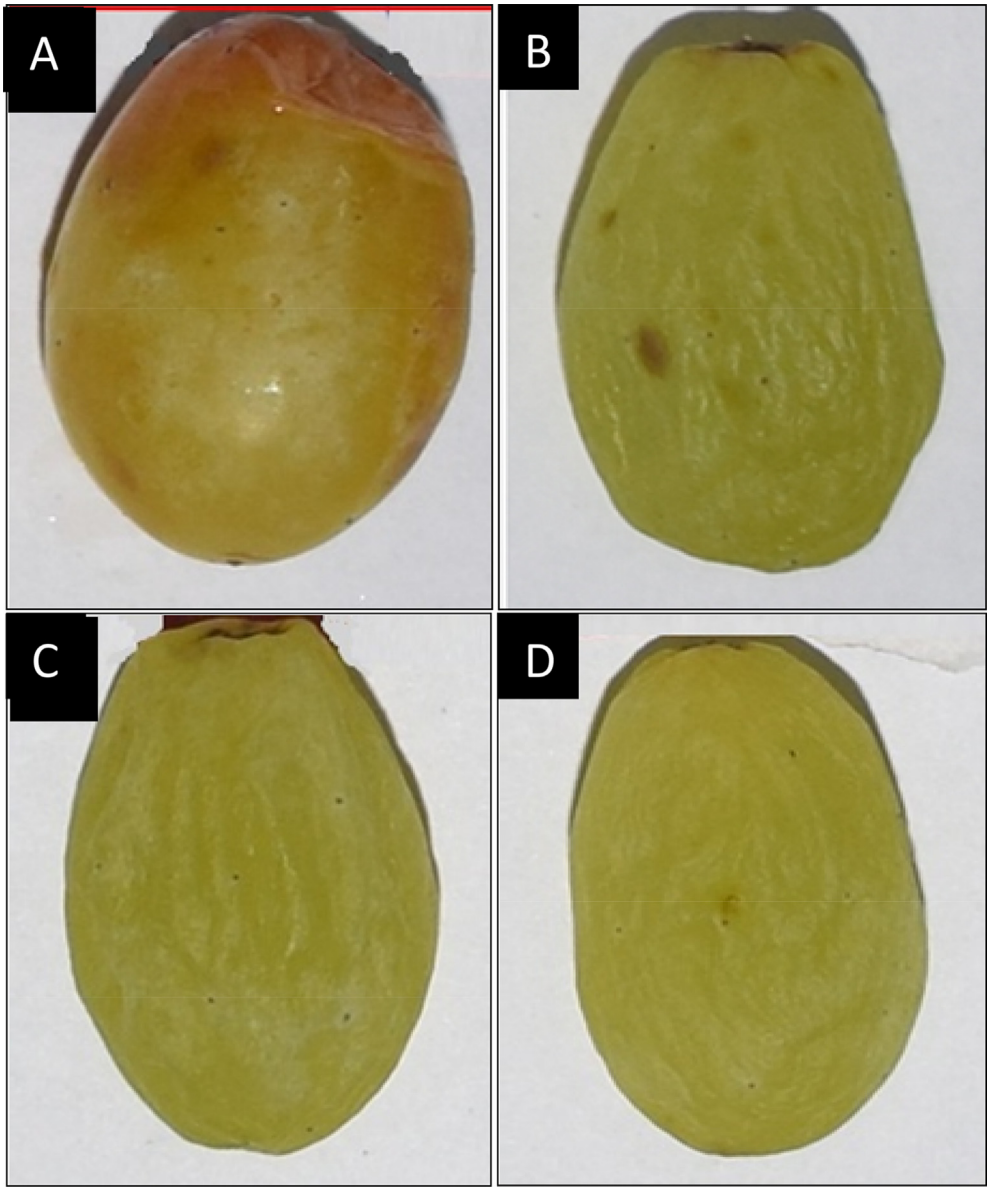

Fig. 7. Images of the green grape wrapped in: (A) Plastic (polyethylene) film, (B) Control film, (C) Film with 2 % (w/w) Agar-ZnO, and (D) Film with 4 % (w/w) agar-ZnO after 9 days storage at 37 °C.

3.2.4. FTIR spectra of the developed films

FTIR spectroscopy of the developed composite film samples was carried out to detect the potential intermolecular interaction among various components of the nanocomposites (Fig. 5). The FTIR spectrum of the only agar film shows characteristic absorption bands at 3317 cm^{-1} attributed to the stretching vibration of the combined peaks of $–NH_2$ and –OH groups, bands at 2922 cm^{-1} attributed to asymmetric stretching of $–CH_3$, peaks at 1637 cm^{-1} ascribed to bending vibration of $–NH_2$ group and stretching vibration of –C=*O group* (Tako et al., 1999). The 1368 cm^{-1} band was attributed to the $–CH_3$ symmetrical deformation mode and the absorption bands at 1155 cm^{-1} and 1042 cm^{-1} are ascribed to the C–O stretching vibrations (C–O–C) of aliphatic ether. Comparing the IR spectra of the control film with the agar-ZnONPs composite films, it is evident that the peak intensities of the agar-ZnONPs composite films were reduced than those of the control. However, the peak positions remained unchanged. The results suggest that there are no major structural changes in the nanocomposites.

3.2.5. Thermal properties of the nanocomposites

The nanocomposites exhibit four steps of weight loss in thermogravimetry studies (Fig. 6). Between 50°–150 °C, the weight loss is due to moisture removal, while the weight loss around 150°–225 °C can be attributed to the thermal degradation of plasticizer (glycerol) in the composite films (Sadeghi and Shahedi, 2016). The weight losses at 225°–300 °C and 300°–500 °C can be ascribed to the removal of organic functional groups from the agar matrix. Similar thermal decomposition of agar polymer was reported by El-Hefian et al., 2012. In case of control (only agar) film, the maximum weight loss was observed at about 225 °C, whereas in case of the composite films, it was at approximately 245 °C indicating higher thermal stability of the ZnONPs incorporated nanocomposite films.

3.3. Effectiveness of the developed film in packaging of green grape

The effectiveness of the composite films as packaging material for green grapes was studied. Visual observations are shown in Fig. 7. The green grapes wrapped in plastic film showed clear mildew appearance with several moldy spots on surface after 7-days of storage. Sticky juice also leaked from the fruit (Fig. 7A) along with a strong rotten smell. Whereas, in case of control film, the mildew appearance was shown only on upper end and a few yellowish spots on the surface of the grape were seen after 7-days storage (Fig. 7B). The fruits wrapped in agar-ZnO nanocomposite films were still visibly fresh with acceptable visual appearance (Fig. 7C & D). The appearance of the green grapes remained acceptable after being wrapped in nanocomposite film with 2 % (w/w) of ZnONPs for 14-days, whereas it lasted for 21-days when wrapped in film with 4 % (w/w) of ZnONPs. It was observed that the efficiency of preservation of grapes were directly proportional to the concentration of NPs in agar-ZnONPs matrix. The results showed that the fabricated composite film could be a promising material for packaging of green grapes, which may be evaluated further in future studies.

4. Conclusions

This study demonstrates the green synthesis of ZnO NPs using fruit extract of *Mimusops elengi* and its application in fabrication of nanocomposite films with desired properties. The diameter of synthesized nanoparticles were 14–48 nm of hexagonal shapes. Thermal stability, elongation at break and fruit preservation properties of the nanocomposite films were enhanced upon adding ZnONPs in the agar matrix. The green grapes wrapped in the developed films remained acceptable in appearance for extended periods in ambient storage. Thus, the fabricated nanocomposite film could be used as an effective packaging material for shelf-life extension of green grapes. Further characterization such as gas and moisture barrier properties, antimicrobial activity, etc. may be explored in future research work.

Declarations

Author contribution statement

Santosh Kumar: Conceived and designed the experiments; Analyzed and interpreted the data; Contributed reagents, materials, analysis tools or data; Wrote the paper.

Jyotish Chandra Boro 2 3: Performed the experiments; Analyzed and interpreted the data.

Dharitri Ray: Performed the experiments.

Avik Mukherjee: Analyzed and interpreted the data; Contributed reagents, materials, analysis tools or data; Wrote the paper.

Joydeep Dutta: Conceived and designed the experiments; Wrote the paper.

Funding statement

This research did not receive any specific grant from funding agencies in the public, commercial, or not-for-profit sectors.

Competing interest statement

The authors declare no conflict of interest.

Additional information

No additional information is available for this paper.

Acknowledgements

SK is very much thankful to Department of Biotechnology, Government of India for providing financial support (sanction letter vide no. BT/20/NE/2011) to peruse post-doctoral research at Functional Materials, KTH Royal Institute of Technology, Stockholm, Sweden through “Biotechnology Overseas Associateship Award for NER Scientists”.

References

Al-Naamani, L., Dobretsov, S., Dutta, J., 2016. Chitosan-zinc oxide nanoparticle composite coating for active food packaging applications. Innov. Food Sci. Emerg. Technol. 38, 231–237.

Al-Naamani, L., Dobretsov, S., Dutta, J., Burgess, J.G., 2017. Chitosan-zinc oxide nanocomposite coatings for the prevention of marine biofouling. Chemosphere 168, 408–417.

Ali, Y., Jasim, A., Jacob, A.H., 2017. Preparation and characterization of agar-based nanocomposite films reinforced with bimetallic (Ag-Cu) alloy nanoparticles. Carbohydr. Polym. 155, 382–390.

Baliga, M.S., Pai, R.J., Bhat, H.P., Palatty, P.L., Boloor, R., 2011. Chemistry and medicinal properties of the Bakul (*Mimusops elengi* Linn): a review. Food Res. Int. 44, 1823–1829.

Bhuyan, T., Mishra, K., Khanuja, M., Prasad, R., Varma, A., 2015. Biosynthesis of zinc oxide nanoparticles from *Azadirachta indica* for antibacterial and photocatalytic applications. Mater. Sci. Semicond. Process. 32, 55–61.

Bora, T., Sathe, P., Laxman, K., Dobretsov, S., Dutta, J., 2017. Defect engineered visible light active ZnO nanorods for photocatalytic treatment of water. Catal. Today 284, 11–18.

Chauhan, S., Upadhyay, M.K., Rishi, N., Rishi, S., 2011. Phytofabrication of silver nanoparticles using pomegranate fruit seeds. Int. J. Nano Biomaterials (IJNBM) 1, 17–21.

Çolak, H., Karakose, E., 2017. Green synthesis and characterization of nanostructured ZnO thin films using *Citrus aurantifolia* (lemon) peel extract by spin-coating method. J. Alloy. Comp. 690, 658–662.

Davar, F., Majedi, A., Mirzaei, A., 2015. Green synthesis of ZnO nanoparticles and its application in the degradation of some dyes. J. Am. Ceram. Soc. 98 (6), 1739–1746.

EFSA CEF Panel On food contact materials, EU, flavourings and processing aids, 2015. Scientific Opinion on the safety evaluation of the substance zinc oxide, nanoparticles, uncoated and coated with [3-(methacryloxy)propyl] trimethoxysilane, for use in food contact materials. EFSA J. 13 (4), 4063–4072.

Ekthammathat, N., Thongtem, S., Thongtem, T., Phuruangrat, A., 2014. Characterization and antibacterial activity of nanostructured ZnO thin films synthesized through a hydrothermal method. Powder Technol. 254, 199–205.

El-Hefian, E.A., Nasef, M.M., Yahaya, A.H., 2012. Preparation and characterization of chitosan/agar blended film: Part-2. Thermal, mechanical, and surface properties. E-J. Chem. 9, 510–516.

Espitia, P.J.P., Otoni, C.G., Soares, N.F.F., 2016. Zinc oxide nanoparticles for food packaging applications. Antimicrobial Food Packaging. Associated Press, USA, pp. 425–431.

Govindaraju, K., Kiruthiga, V., Manikandan, R., Ashokkumar, T., Singaravelu, G., 2011. B-glucosidase assisted biosynthesis of gold nanoparticles: a green chemistry approach. Mater. Lett. 65, 256–259.

Khalil, H.P.S.A., Saurabh, C.K., Tye, Y.Y., Lai, T.K., et al., 2017. Seaweed based sustainable films and composites for food and pharmaceutical applications: a review. Renew. Sustain. Energy Rev. 77, 353–362.

Kumar, S., Singh, M., Halder, D., Mitra, A., 2016. *Lippia javanica*: a cheap natural source for the synthesis of antibacterial silver nanocolloid. Appl. Nanosci. 6, 1001–1007.

Kumar, S., Mitra, A., Halder, D., 2017. *Centella asiatica* leaf mediated synthesis of silver nanocolloid and its application as filler in gelatin based antimicrobial nanocomposite film. LWT - Food Sci. Technol. (Lebensmittel-Wissenschaft -Technol.) 75, 293–300.

Kumar, S., Shukla, A., Baul, P.P., Mitra, A., Halder, D., 2018. Biodegradable hybrid nanocomposites of chitosan/gelatin and silver nanoparticles for active food packaging applications. Food Packag. Shelf Life 16, 178–184.

Kumar, H.A.K., et al., 2014. Antimicrobial and antioxidant activities of *Mimusops elengi* seed extract mediated isotropic silver nanoparticles. Spectrochim. Acta Mol. Biomol. Spectrosc. 130, 13–18.

Kumari, R., Brahma, G., Rajak, S., Singh, M., Kumar, S., 2016. Antimicrobial activity of green silver nanoparticles produced using aqueous leaf extract of *Hydrocotyle rotundifolia*. Orient. Pharm. Exp. Med. 16, 195–201.

Malagurski, I., Levic, S., Nesic, A., Mitric, M., et al., 2017a. Mineralized agar-based nanocomposite films: potential food packaging materials with antimicrobial properties. Carbohydr. Polym. 175, 55–62.

Malagurski, I., Levic, S., Pantic, M., Matijasevic, D., Mitric, M., Pavlovic, V., Dimitrijevic-Brankovic, S., 2017b. Synthesis and antimicrobial properties of Zn-mineralized alginate nanocomposites. Carbohydr. Polym. 165, 313–321.

Mitra, R., 1981. Bakula- A reputed drug of Ayurveda, its history, uses in Indian medicine. Indian J. Hist. Sci. 12, 169–180.

Orsuwan, A., Shankar, S., Wang, L.F., Sothornvit, R., Rhim, J.W., 2016. Preparation of antimicrobial agar/banana powder blend films reinforced with silver nanoparticles. Food Hydrocolloids 60, 476–485.

Rashad, M.M., Ismail, A.A., Osama, I., Ibrahim, I.A., Kandil, A.H.T., 2014. Photocatalytic decomposition of dyes using ZnO doped SnO_2 nanoparticles prepared by solvothermal method. Arabian J. Chem. 7 (1), 71–77.

Reddy, J.P., Rhim, J.W., 2014. Characterization of bionanocomposite films prepared with agar and paper-mulberry pulp nanocellulose. Carbohydr. Polym. 110, 480–488.

Rhim, J.W., Wang, L.F., 2013. Mechanical and water barrier properties of agar/carrageenan/konjacglucomannan ternary blend biohydrogel films. Carbohydr. Polym. 96, 71–81.

Sadeghi, K., Shahedi, M., 2016. Physical, mechanical, and antimicrobial properties of ethylene vinyl alcohol copolymer/chitosan/nano-ZnO (ECNZn) nanocomposite films incorporating glycerol plasticizer. J. Food Meas. Charact. 10, 137–147.

Santana, T.J.M., Pelegrín, Y.F., Barrios, J.A.A., 2014. Physicochemical and morphological properties of plasticized poly(vinyl alcohol)–agar biodegradable films. Int. J. Biol. Macromol. 69, 176–184.

Santhoshkumar, J., VenkatKumar, S., Rajeshkumar, S., 2017. Synthesis of zinc oxide nanoparticles using plant leaf extract against urinary tract infection pathogen. Resour. Efficient Technol. 3, 459–465.

Shah, P.J., Gandhi, M.S., Shah, M.B., Goswami, S.S., Santani, D., 2003. Study of *Mimusops elengi* bark in experimental gastric ulcers. J. Ethnopharmacol. 89, 305–311.

Spierling, S., Knüpffer, E., Behnsen, H., Mudersbachet, M., et al., 2018. Bio-based plastics - a review of environmental, social and economic impact assessments. J. Clean. Prod. 185, 476–491.

Stan, M., Popa, A., Toloman, D., Dehelean, A., Lung, I., Katona, G., 2015. Enhanced photocatalytic degradation properties of zinc oxide nanoparticles synthesized by using plant extracts. Mater. Sci. Semicond. Process. 39, 23–29.

Tako, M., Higa, M., Medoruma, K., Nakasone, Y., 1999. A highly methylated agar from red seaweed, *Gracilaria arcuata*. Bot. Mar. 42, 513–518.

Tee, T., Hui, S.T.C., Yi, C.W., Chin, Y.C., Umar, A.A., Titian, G.R., Salleh, M.M., 2016. Microwave-assisted hydrolysis preparation of highly crystalline ZnO nano rod array for room temperature photoluminescence-based CO gas sensor. Sensor. Actuator. B Chem. 227, 304–312.

Tian, T., Xing, J., Cheng, L., Zheng, L., Ruan, W., Ruan, X., Li, G., 2015. Synthesis of large size ZnO micro rods by a simple way of thermal evaporation. Ceram. Int. 41, S774–S778.

Vakulov, Z.E., Zamburg, E.G., Khakhulin, D.A., Ageev, O.A., 2017. Thermal stability of ZnO thin films fabricated by pulsed laser deposition. Mater. Sci. Semicond. Process. 66, 21–25.

Zare, E., Pourseyedi, S., Khatami, M., Darezereshki, E., 2017. Simple biosynthesis of zinc oxide nanoparticles using nature's source, and it's in vitro bio-activity. J. Mol. Struct. 1146, 96–103.